Journal of Alloys and Compounds 509 (2011) 4025–4034

Contents lists available at ScienceDirect

Journal of Alloys and Compounds

journal homepage: www.elsevier.com/locate/jallcom

Elastic fields generated by a semi-spherical hydride particle on a free surface of a metal and their effect on its growth

Y. Greenbaum [a], D. Barlam [b], M.H. Mintz [a,d], R.Z. Shneck [c,*]

[a] Department of Nuclear Engineering, Ben-Gurion University of the Negev, Beer Sheva, P.O. Box 653, Israel
[b] Department of Mechanical Engineering, Ben-Gurion University of the Negev, Beer Sheva, P.O. Box 653, Israel
[c] Department of Materials Engineering, Ben-Gurion University of the Negev, Beer Sheva, P.O. Box 653, Israel
[d] Nuclear Research Center-Negev, P.O. Box 9001, Beer Sheva, Israel

ARTICLE INFO

Article history:
Received 24 November 2010
Received in revised form
30 December 2010
Accepted 3 January 2011
Available online 6 January 2011

Keywords:
Metal hydride
Precipitation
Anisotropy
Diffusion
Computer simulations
Thermodynamic modeling

ABSTRACT

The formation of a metal hydride is associated with a large increase of volume relative to the parent metal and therefore in large strain energies. Effects of elastic energy on the hydriding of metals are revealed in the microstructural evolution and kinetics of hydride growth on free surfaces. In the present work, we study in detail the elastic fields set up by a semi-spherical hydride particle growing at a free surface of metal with cubic symmetry, with and without an oxide layer. These systems combine geometric (structural) and material anisotropies.

Three stages along the microstructural evolution on the surface of some hydride forming metals exposed to hydrogen at constant pressure were described experimentally. For these stages along hydride growth, correlations with the elastic fields are suggested as follows. (a) A hydride particle at the free surface generates regions of tensile and compressive hydrostatic stress in the surrounding matrix. This may induce a preferred nucleation of new hydrides and formation of clusters of hydrides precipitates, which is indeed observed experimentally. (b) Clustering, on the other hand, may contribute to the cease of growth due to competition on hydrogen. In addition, as the particle grows, changes in the stress fields may retard further diffusion from the surface and be another contribution to the cease of growth. (c) A growing hydride increases the stress in the oxide layer and may finely break it. Then the elastic energy per unit volume drops to its minimum value and the growth may accelerate. The formation of such "growth center" is favored for that hydride precipitate that grow alone and not in a cluster.

1. Introduction

The formation of a metal hydride is associated with a large increase of volume relative to the parent metal. It is possible to measure this volume change from the difference between the lattice parameters of the metal and the hydride. Recently the bending of thin films of palladium was utilized to directly measure the internal stresses due to this volume change [1]. The elastic energy accompanying the hydride particles growth on metal surfaces may be of the same magnitude as that of the chemical driving force of hydride formation and therefore it may have a significant effect on the reaction characteristics. The influence of the strain energy on hydriding of metals is manifested by several phenomena. The two most common effects are the pulverization of bulk metals during repeated hydriding/dehydriding cycles and hysteresis of the pressure-composition absorption/desorption isotherms. Surface relief, buckling and cracking [2,3] that lead to the pulverization [e.g. [4,5]] are means to relieve the elastic stresses that are set up by the hydrides. The hysteresis is attributed to the suppression of the absorption of hydrogen by the additional strain energy effect. There is a long standing controversy whether it is the plastic energy [6–9] or the elastic energy [2,10,11] that is responsible for the hysteresis and whether the measurements reflect a real thermodynamic equilibrium or a kinetic effect [12,13]. Fundamental, yet less studied aspects of the influence of the strain energy are its effects on the microstructure evolution and on the kinetics and dynamics of the hydriding and dehydriding processes. Theoretically, the elastic energy of a dilating second phase on a free surface is minimal when the shape of the particle is semi-spherical [14]. This prediction is apparently confirmed by experimental observation at the early stages of hydriding [15]. In the case of $ZrH_{1.5}$ definite orientation relations and texture of hydrides were observed that indicate an effect of elastic stresses [16]. A much more complicated aspect is the kinetics and dynamics of the hydriding and dehydriding. These processes are associated with diffusion through three phases: surface oxides, the reacting metal and the hydride, under the effects of significant stress fields. Several kinetic models of the hydriding/dehydriding disregard these stress effects [17–19]. Recently

* Corresponding author. Tel.: +972 8 6472493; fax: +972 8 6472946.
E-mail address: roni@bgu.ac.il (R.Z. Shneck).

0925-8388/$ – see front matter © 2011 Elsevier B.V. All rights reserved.
doi:10.1016/j.jallcom.2011.01.010

a phase-field model was developed to simulate the morphology evolution of hydride precipitation that considers the elastoplastic behavior of zirconium bulk matrix [20]. The kinetics of hydriding of metal nanoparticles where the stresses are already small was analyzed by Zhdanov [13]. In a recent study [21] a complete wave-like dynamics of adsorbed hydrogen were attributed to stress related phenomena.

Several experimental observations [15,22,23] described the microstructural evolution and kinetics of hydrides growth on surfaces. Initially, many small sub-micron hydride precipitates are nucleated and tend to cluster. These precipitates are formed rapidly but their growth rate strongly decelerates. Following this stage a few of these hydrides are observed to start growing very fast in an irregular manner (referred to as "growth centers") [23] until they cover the whole surface.

In the present work, we describe and analyze the elastic fields set up by a semi-spherical hydride particle growing on a free surface of a metal with a cubic symmetry and try to interpret their influence on the evolution of the microstructure and on some kinetic characteristics of the growing hydride precipitates. The elastic anisotropy turns to have an important effect on the elastic fields, and the cubic symmetry was chosen for its simplicity and abundance. This system combines geometric (a free surface) and material (cubic symmetry) anisotropies; therefore, we develop our understanding gradually. First, a spherical particle growing in an infinite isotropic matrix is described and compared to a semi-spherical particle on a free surface. Second, a spherical particle growing in an infinite matrix with cubic symmetry is described and compared to a semi-spherical particle growing on a free surface of the same cubic material. Third, the contribution of an oxide layer coating the surface on the stress fields set up by the hydride that grows underneath is studied.

The interaction of the hydride with solute hydrogen atoms in the metal matrix is proportional to the hydrostatic stress set by the hydride on its surroundings [24]. This stress component will affect the supply of hydrogen by diffusion to the hydride and the preference for nucleation of other hydride particles near the initial precipitate [25]. Therefore, in the following analysis emphasis will be given first to find and understand the variation of the hydrostatic stress component around the hydride and second to determine the variation of the total elastic energy with varying of the size of the hydride relative to the thickness of the covering oxide layer.

The outcome of the above analysis is the understanding of the contribution of the mechanical energy to the initial stages of development of hydrides. This includes the very initial nucleation and growth processes where dense hydride "spots" are formed, with decaying growth rates, a clustering tendency [15] and the following development of fast growing hydride "patches" ("growth centers") that finally coat the surface [23]. It is shown that these development characteristics can be accounted for by the mechanical energy contributions.

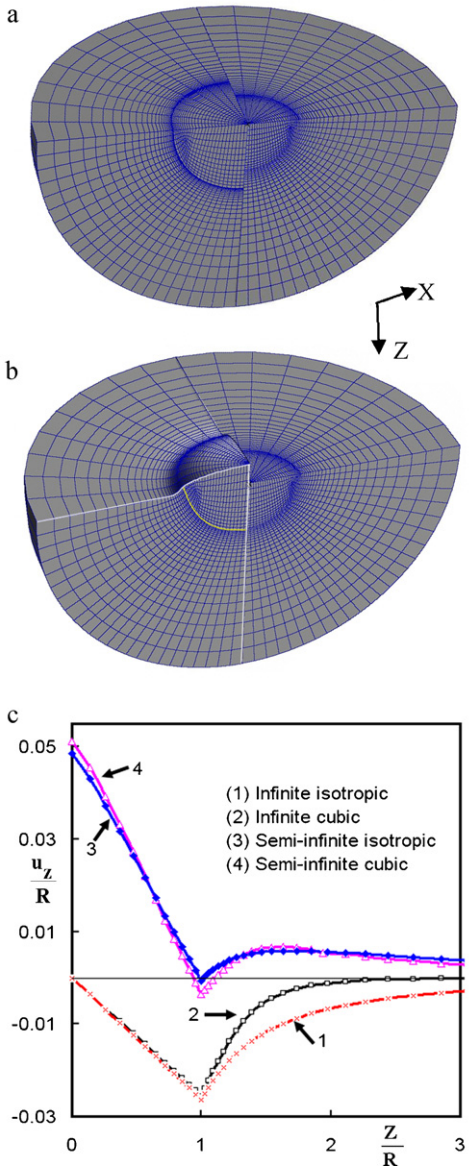

Fig. 1. Displacements of isotropic infinite and semi-infinite systems. Comparison of the displacements due to the formation of a semispherical hydride particle: (a) in an infinite matrix (left half), compared to the reference state before the reaction (right half), (b) on a free surface (left half), compared to the reference state before the reaction and (c) displacement profiles u_z along the z-axis for infinite and semi-infinite systems, for isotropic and cubic materials. The negative displacement indicates displacement out of the free surface, positive one creates compression relative to the stress free state.

2. Method of calculation

The calculations were performed by the FEM applying the MSC.NASTRAN [26] code. A 180° spherical segment was modeled. A hydride is assumed to have a semi-spherical shape (see Fig. 1). Both isotropic and cubic symmetries are considered. For anisotropic systems, the crystallographic axes of the matrix and precipitate are assumed parallel to each other. Pure dilatational (misfit) transformation strains are assumed ($\varepsilon_{ij}^{T} = \varepsilon^{0}\delta_{ij}$) and represented as thermal strains in the hydride.

The elastic constants selected for the specific model system of Pd–H are listed in Table 1. For the isotropic cases, the properties of polycrystalline palladium are used for both the metal and its hydride. For the system with cubic symmetry, the elastic constants of single crystal palladium were chosen for the matrix and those of $PdH_{0.6}$ were used for the hydride. The constants of the oxide layer were those measured for PdO. The linear misfit value was calculated from the hydride and metal densities [27] and found to be $\varepsilon_L^0 = 0.034$.

Table 1
The elastic constants of the materials used in the models, calculated from the cited references.

Material	C_{11} (GPa)	C_{12} (GPa)	C_{44} (GPa)	A
Pd single cryst. [27]	224	173	71.25	2.8129
$PdH_{0.6}$ [27]	211	156	63.45	2.4720
PdO [28]	339.1	216.8	61.15	1
Pd polycrystal [29]	241.36	154.31	43.52	1

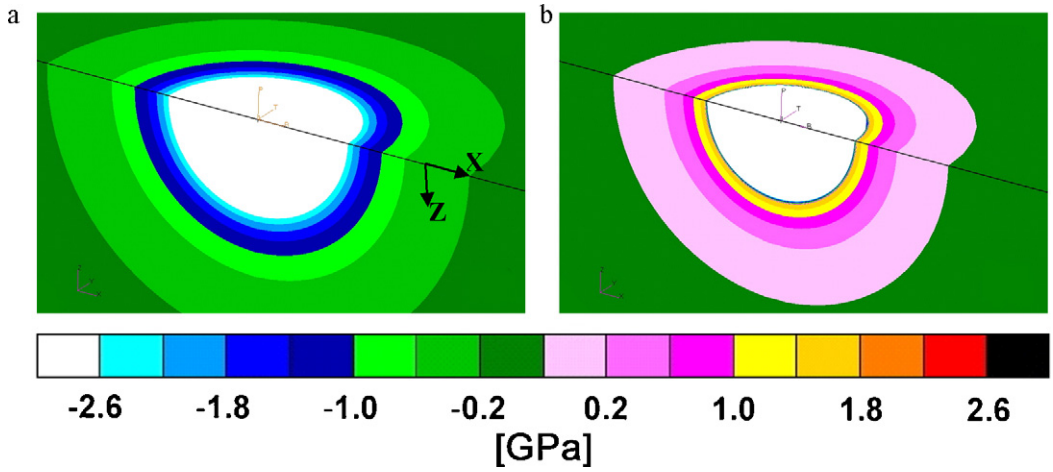

Fig. 2. Stress maps of the matrix affected from a spherical hydride particle *embedded in infinite* matrix, assuming *isotropic* material behavior. (a) Radial stress σ_{rr}, (b) tangential stresses $\sigma_{\theta\theta} = \sigma_{\phi\phi}$ (negative stress values indicate compression, positive ones indicate dilation). The hydrostatic pressure is zero in the matrix. The stress map is truncated above ±3.0 GPa, in order to keep uniform scale in all the stress figures in this work.

3. Results

3.1. Isotropic material

3.1.1. Kinematics of a hydride

The formation of a hydride particle is associated with volumetric dilation relative to the metal matrix. In the following discussion, it is assumed that all the misfit strains induced by the hydride development are within the elastic regime and that a coherent interface is maintained between the hydride and the surrounding metal matrix. Within these assumptions, if the hydride is formed in a spherical cavity in an infinite matrix – a state of pure hydrostatic stresses prevails in the hydride [24]. In the following, we shall study the kinematics of a *hydride particle* that grows in a semi-spherical cavity at a *free surface* (Fig. 1) and compare the displacement's set up in a hydride that grows on a free surface of a metal matrix to that in an infinite matrix. All the lattice lines in the hydride particles elongate during the dilations accompanying the hydrogenation of the matrix. Fig. 1a shows that all the radial lines within a spherical hydride embedded in infinite matrix are elongated radially outwards. Fig. 1b shows that the elongation near a free surface is achieved by *bending* of the lines toward the free surface. The bending out becomes possible by two complementary properties of a half space relative to an infinite matrix: the elimination of half of the matrix removes constraints on displacements at the free surface, mainly normal to that surface and the tractions on the free surface vanish due to the free boundary conditions.

Two competitive effects govern the kinematics of the *matrix* points below the hydride: (a) the dilatation of the new phase causes compression of the surrounding matrix and (b) the dilatation in the hydride is obtained by bending of its lattice lines. Due to the second effect, the hydride pulls the surrounding matrix material outwards, toward the free surface. Since the hydride near a free surface is relatively relaxed, its compression is of a moderate magnitude and of a shorter range than the pulling effect. Fig. 1c describes the radial displacements along the axis normal to the surface z, in infinite and semi-infinite systems. Line 1 shows the displacements in infinite matrix. The displacements are always negative, meaning outwards from the center of the sphere toward the matrix. Line 2 shows the displacements in semi-infinite matrix. They are always positive, meaning that all the hydride points along the z-axis below the free surface are displaced outwards, toward the free surface. At the hydride–metal interface, the compression and the pulling effects are found to nearly balance each other, so that the displacement of the interface relative to its position before the phase transformation is minimal. Further in the matrix, all the displacements are oriented outwards, namely the matrix is pulled toward the free surface. The displacements reach a maximum and then decrease, meaning that in this region the matrix is elongated in the radial direction. This situation is contrary to the intuitive view of a compressive radial field set up by an embedded particle on the surrounding matrix.

3.1.2. Stresses

Figs. 2–4 compare the stresses set up by a hydride in an infinite matrix (Fig. 2) to those at a free surface (Fig. 3). Fig. 3a shows that the radial stress σ_{rr} is compressive in the hydride at a free surface and in the adjacent matrix, but this component quickly decays and turns into tensile stress further along the z axis, as expected from the variation of the radial displacements. We interpret this as a result of the steeper decay of the compressive effect relative to the bending or pulling effect that becomes dominant. Parallel to the free surface, the radial stresses within the hydride are greatly relaxed (Fig. 4a). This is an indication that the hydride material has undergone large elongation near the surface. This elongation of the hydride cause large radial compression in the ring-shaped region of the matrix, peripheral to the hydride (Fig. 3a). Due to the continuity of the radial stress component through the hydride–matrix interface, the radial stress along the free surface is gradually building up from the hydride into the ring shaped region in the matrix, and it decays away farther from the hydride (Fig. 4a).

In the interior of the matrix, the tangential stresses $\sigma_{\theta\theta}$ and $\sigma_{\phi\phi}$ are everywhere tensile and since the compressive term σ_{rr} is small, the hydrostatic stress (which is the sum of these normal stress components) is tensile (Figs. 3b–d and 4). On the free surface, the tangential stress $\sigma_{\phi\phi}$ appears similar to this component in an infinite matrix (Figs. 2b and 3c), whereas $\sigma_{\theta\theta}$ that is normal to the free surface, decays to zero to conform to the boundary conditions (Fig. 3d). The hydrostatic stress is compressive only near the free surface, governed by the compressive radial stress in the ring-shaped region around the hydride.

3.2. Anisotropic cubic material

3.2.1. Radial stresses

The response of materials with cubic symmetry is different along different directions. The elastic fields associated with a dilating hydride in an *infinite* matrix is modified to a small extend by the cubic anisotropy. Most metals have anisotropy factor $A = 2C_{44}/(C_{11} - C_{12}) > 1$. In these metals the elastic constant C_{11} is minimal along <1 0 0> directions, maximal along <1 1 1> directions

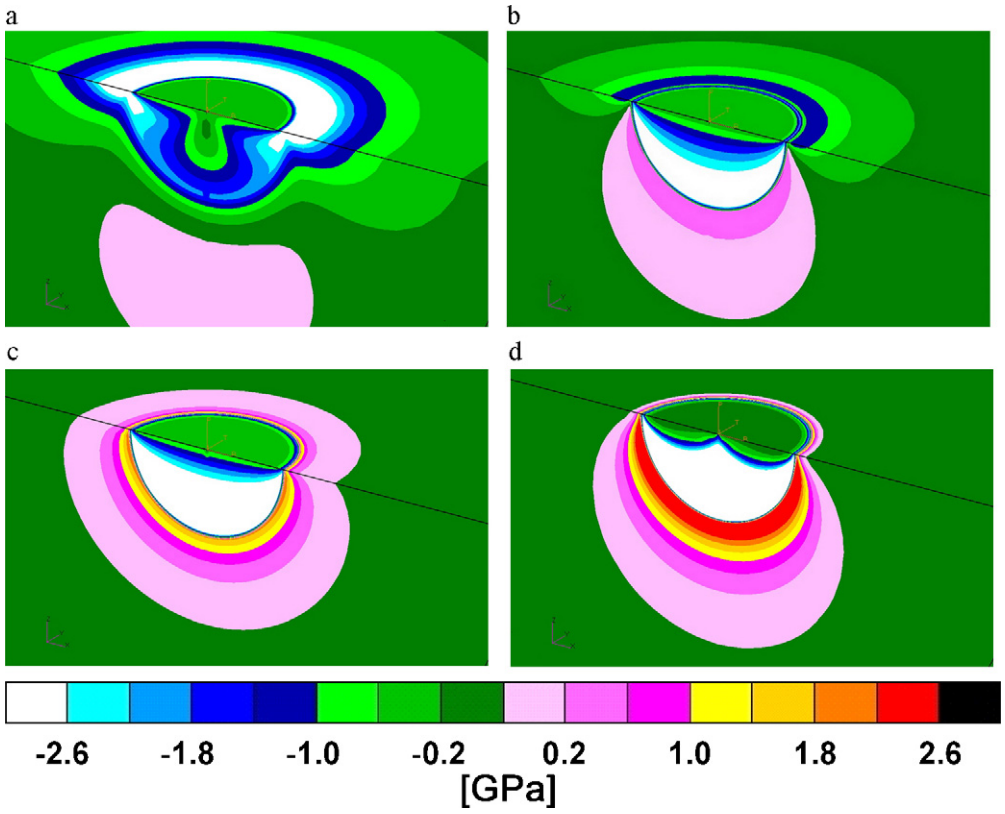

Fig. 3. Stress maps generated by a semi-sphrical hydride particle tangent to the free surface, assuming *isotropic* material behavior. (a) radial stress – σ_{rr}, (b) hydrostatic pressure – P, (c) tangential stresses – $\sigma_{\phi\phi}$ and (d) $\sigma_{\theta\theta}$.

and have saddle points along the <1 1 0> directions. Thus, if identical *strains* have been enforced on all the material elements at equal distances from the hydride particle, then the *stresses* were not equal. Larger normal stresses would be created along the harder directions that have the larger elastic constant C_{11}, and smaller stresses would be created along the soft directions, those with smaller elastic constant. Therefore the material response is to have smaller radial compressive strains along the hard <1 1 0> and <1 1 1> directions and larger strains along the soft <1 0 0> directions.

Beginning with an infinite system, the radial strains in the matrix accommodate the 'hydride dilation'. Along the soft directions, large radial compressive strains allow accumulating most of the hydride boundary displacement within a small region of the matrix near the hydride boundary (Fig. 5a), therefore the outward displacements in the matrix shortly diminish. Along the hard <1 1 1> and <1 0 1> directions in the matrix *smaller* strains are allowed but they have to accommodate *similar* displacements of the hydride boundary. In order to accommodate these displacements, the small compressive strains along the hard directions have to sustain a longer distance from the interface. Therefore, the radial displacements sustain farther from the interface. This anisotropy of the radial elastic strain in an infinite cubic matrix has already been described [30].

The anisotropy on the *free surface* that is parallel to the crystallographic plane (0 0 1) looks very similar to this plane in an *infinite* matrix (compare Figs. 6–8Figs. 6a and 7a and 8). The radial stress is large and sustain for a long range along the hard <1 1 0> directions. It has a smaller range along the soft <1 0 0> direction. The radial stress distribution along the normal to the free surface (Fig. 7a) has been interpreted in the previous section as an outcome of two competing effects: compression due to the dilatation and pulling out due to line bending and relaxation. The radial stress is largely relaxed in the z direction normal to the free surface already in isotropic materials (Fig. 3a). In cubic materials, the compression effect decays quicker along the normal to the free surface, since it is also a soft direction. Hence, the remaining pulling out effect appears closer and stronger, compared with an isotropic material (Figs. 2a, 3a, 6a and 7a).

3.2.2. Tangential stresses

The tangential stresses around the spherical precipitate embedded in an infinite matrix with cubic symmetry are shown in Fig. 6c and d. They are due to the elongation of the particle–matrix interface. A spherical dilating particle remains spherical when it is embedded in an *infinite matrix* [24], therefore, the elongation of the hydride–matrix interface is uniform. Fig. 6c shows the $\sigma_{\phi\phi}$ component of stress in the (0 0 1) plane. Despite the uniform elongation of the interface, $\sigma_{\phi\phi}$ depends on its crystallographic orientation: it is large when oriented along a <1 1 0> hard direction and small when it is oriented along a <1 0 0> soft direction. Fig. 6d shows the $\sigma_{\theta\theta}$ component. It is oriented along the [0 0 1] crystallographic direction all over the (0 0 1) the plane (shown by an arrow in Fig. 6d). $\sigma_{\theta\theta}$ is related to the strain $\varepsilon_{\theta\theta}$ by the elastic modulus C_{11}, which has a constant value in the [0 0 1] orientation. Yet the stress is *not* uniform around the particle in the (0 0 1) plane. This demonstrates a non-local variation of the stresses in anisotropic materials: the stresses are influenced by neighboring material elements as well, as will be shown in the next section.

Along the soft <1 0 0> directions, there are small tensile tangential stresses near the hydride–matrix boundary, but they sustain a long distance from the hydride. Along the hard <1 1 0> directions the stresses are larger at the boundary but sustain a shorter range (Fig. 6c and d). As explained in Section 3.2.1, along the hard directions the material is displaced radialy outwards more than along a soft <1 0 0> direction. One notes that each <1 0 0> direction is surrounded by four hard <1 1 0> directions and four hardest <1 1 1> directions (Fig. 5c). Therefore along these soft <1 0 0> directions the

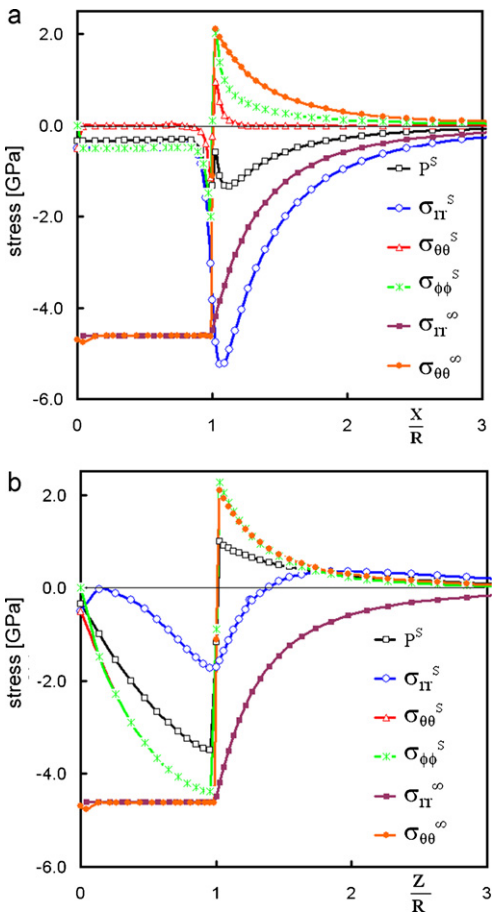

Fig. 4. Profiles of the stress components for infinite and semi-inifinte (surface) systems and isotropic material behavior. (a) *X* direction and (b) *Z* direction (the semi-infinite, surface case, is denoted by *S*, wheres the infinite case by ∞).

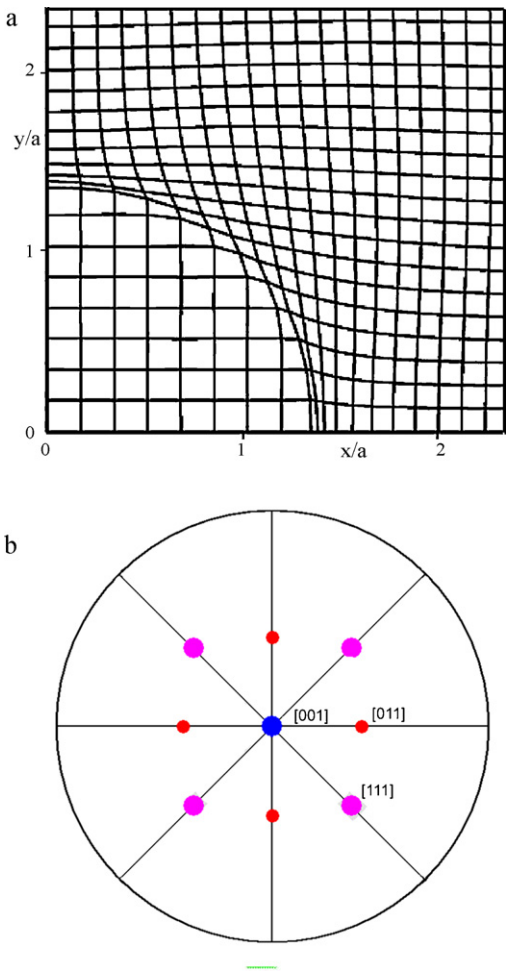

Fig. 5. (a) Displacements associated with a dilating hydride in an infinite matrix. (b) A stereographic projection along the [0 0 1] axis shows the mutual relations of the <0 0 1>, <1 1 0> and <1 1 1> directions in a cubic crystal.

material is stretched toward the hard directions in the tangential plane, normal to the <1 0 0> direction. This stretching is nearly uniform in the (0 0 1) plane and has a long range, related to the range of the radial displacements along the hard directions. According to Newton's third law, the material along the hard directions is also stretched toward the soft <1 0 0> directions (see arrows in Fig. 6c). However, each hard <1 1 0> direction is close only to two soft directions (Fig. 5c), therefore the tangential stresses are smaller and have shorter range. Only in certain regions, the tangential stresses are large. In these regions, the $\sigma_{\phi\phi}$ component is oriented along a hard <1 1 0> crystallographic direction and in addition, is oriented toward the two close soft directions.

When a semi-spherical hydride is formed on a *free surface* half of the matrix is removed relative to an infinite matrix and the hydride is largely relaxed. This gives rise, on the one hand, to a great reduction of the radial stresses in the particle and on the other hand to an increase of the particle diameter and of the tangential strains it imposes on the matrix (Fig. 7). The radial stresses are relaxed by a factor of 10 as shown in Fig. 8a. $\sigma_{\theta\theta}$ is zero on the free surface and it is slightly reduced inside the matrix to cope with these boundary conditions (Fig. 7d). The increased tangential strains are apparent by the increase of magnitude of $\sigma_{\phi\phi}$ and its range increases along all the hard directions, both on the free surface and inside the matrix.

Along the <1 0 0> soft directions on the free surface $\sigma_{\phi\phi}$ significantly decreased. This is due to the elimination of half of the hard directions that surround each soft direction in an infinite matrix that eliminates the tangential stretching of the soft directions. Fig. 8 allows a quantitative comparison between all the stress components.

3.2.3. Hydrostatic stresses

Summing the three normal stress components shows that the ring of compressive pressure at the free surface is less compressive than that of the isotropic case (Figs. 3b and 7b) and has lost its cylindrical symmetry. However a wide envelop of tensile hydrostatic stress exists around the hydride below the free surface. It is generally assumed that the hydrostatic stress component derives the stress-assisted diffusion of hydrogen in solids. Thus, Fig. 7b shows the preferred path for diffusion of hydrogen toward growing hydrides. Hydrogen is usually absorbed through the free surface but the diffusion of the hydrogen toward the hydride is preferred also from the interior of the matrix. The nearly uniform hydrostatic tensile stress also favors a conservation of the shape of the hydride. Interestingly it coincides with the fact that a semi-spherical particle is the shape associated with both minimum elastic energy [5] and minimum surface energy.

3.3. A surface covered with oxide layer

3.3.1. Stress fields

It is well known that in "real" systems the metallic surface is coated by an oxidation overlayer with a thickness and composition that depend on the chemical reactivity of the metals, the history

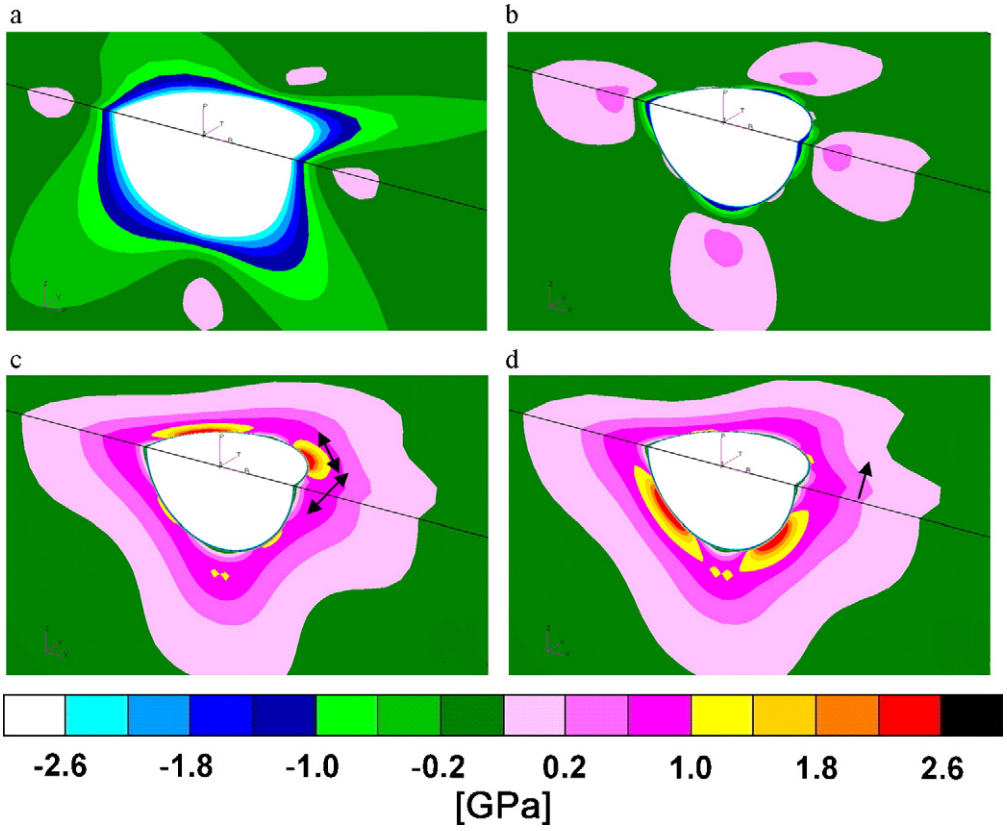

Fig. 6. Stress maps generated by a spherical hydride embedded in *infinite* matrix with *anisotropic* material behavior. (a) σ_{rr}, (b) P, (c) $\sigma_{\phi\phi}$, arrows indicate the [0 1 0] and [1 1 0] directions and (d) $\sigma_{\theta\theta}$, arrow indicates the [0 0 1] direction.

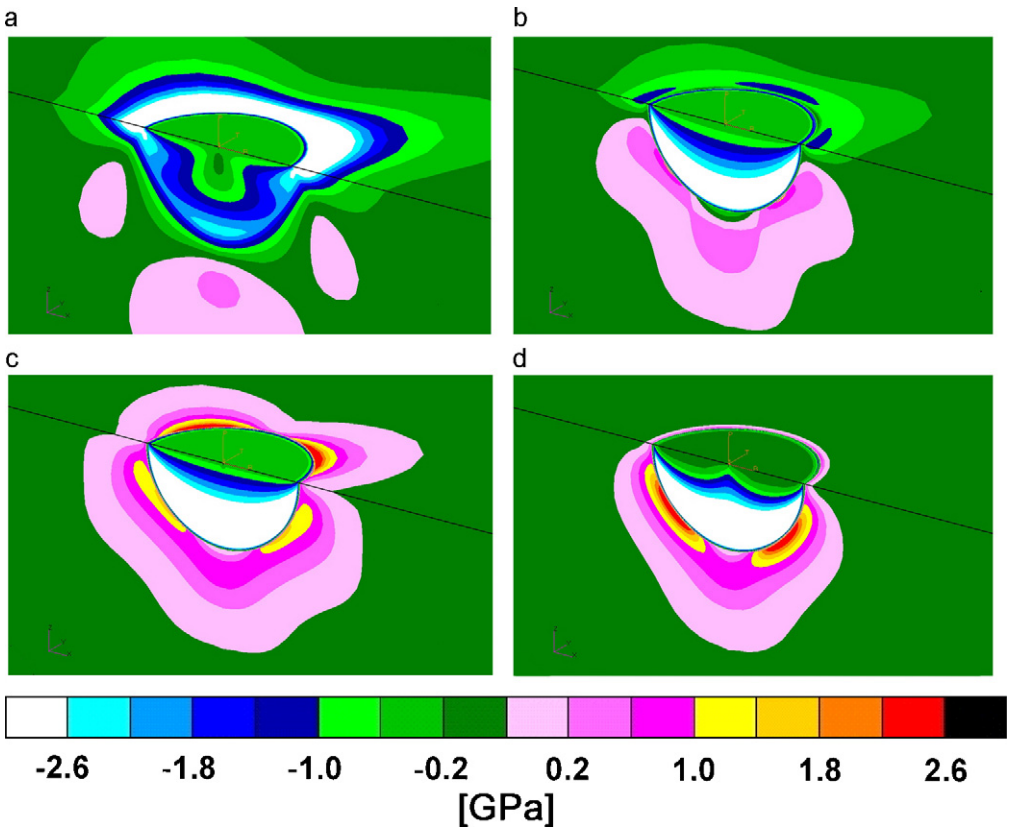

Fig. 7. Stress maps generated by a semi-spherical hydride at a *free surface* with *anisotropic* material behavior. (a) σ_{rr}, (b) P, (c) $\sigma_{\phi\phi}$ and (d) $\sigma_{\theta\theta}$.

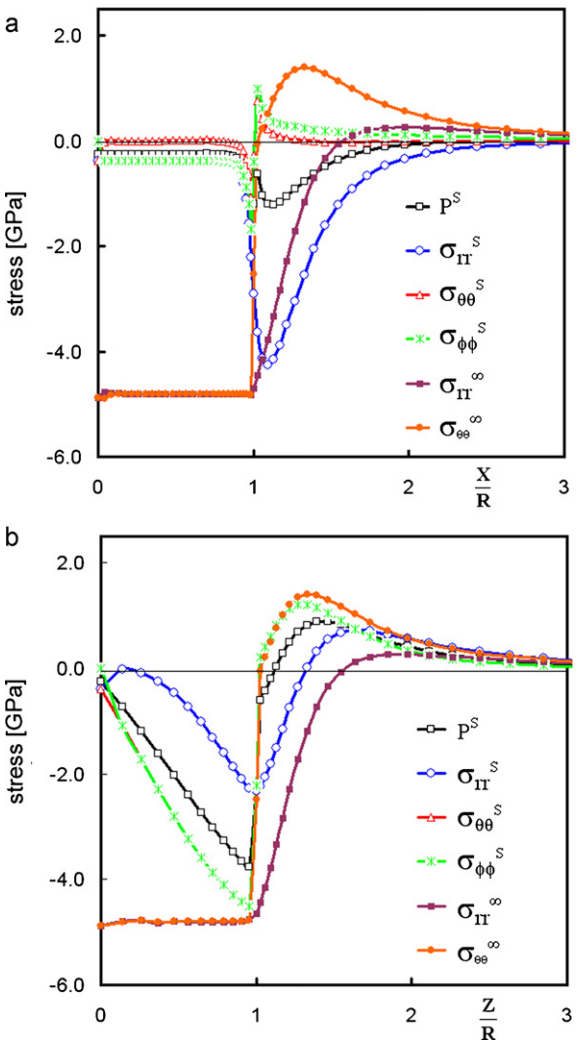

Fig. 8. Profiles of the stress components in infinite and semi-inifinte (surface) systems of anisotropic material. (a) *X* direction and (b) *Z* direction (the infinite case by ∞, the surface case is denoted by *S*).

of its preparation and storage. These oxidation overlayers often impose a barrier for either the dissociative chemisorptions of H_2 on the surface or the penetration of the H atoms across the layer. These effects are manifested by "induction" periods preceding the initiation of the hydride. The chemical or diffusion related effects of oxidation overlayers are of common knowledge (e.g., Ref. [3] and references therein). However, the fact that oxidation overlayers may significantly affect the mechanical energy of hydride nuclei and consequently play an important role in the kinetics and morphology of the development, is scarcely pointed to or treated in the literature.

Oxides are usually stiff elastic materials, thus the existence of a thin oxide layer on a metal surface is expected to constrain the dilation of hydride particles, and to place them closer to the situation of a hydride in an infinite matrix. The tangential stresses in the matrix are determined by expansion of the hydride–matrix interface, therefore the tangential stresses set in the matrix are smaller relative to unoxidized surface (compare Figs. 6, 7 and 9Figs. 6c, 7c and 9c). On the other hand, the radial stresses in the matrix are continuous across the interface. As the compressive stresses in the hydride increase – so do the radial stresses in the matrix that are shifted toward the state of infinite matrix (compare Figs. 6a, 7a and 9a).The additional constraints on the hydride are due to 2D tensile stresses set up in a disk shaped region of the oxide layer on top of the hydride. The hydrostatic pressure in the matrix around a hydride at an oxidized surface is more anisotropic than at unoxidized surface, which resemble more to the pressure distribution in infinite anisotropic matrix (compare Figs. 6b, 7b and 9b). The dilatation in the oxide in a disk-shaped region above the hydride sets up compressive strains in the surrounding oxide. Thus, the ring shaped region of large compressive radial stress that exists around the hydride on a free surface (Fig. 7a), is shifted *into the oxide layer*. This ring gradually disappears when the oxide is relatively thick. In this way, around the hydride a broader tensile pressure ring appears and moves up toward the oxide layer. It has maximum dilation regions at short distances from the hydride–matrix interface along the <1 0 0> axes.

3.3.2. Energetic considerations

Linear elasticity has a linear scaling property. The total elastic energy of the substrate, oxide layer (of thickness t) and a semi-spherical hydride on a free surface (of radius R)with a constant R/t is linearly increasing with the volume of the hydride. The elastic energy of the hydride–metal-oxide system varies with the R/t ratio. This variation is plotted in Fig. 10c. As the hydride grows, it is gradually relaxed and the elastic energy of the system reduces, ultimately when the thickness of the oxide becomes negligible, the energy reduces to the energy of a system containing a hydride on a free surface. Thus, a small hydride particle is constrained to the largest extent and contains large elastic energy. This energy has a maximum retarding effect on the hydride growth. If however it succeeds to grow, the elastic energy per unit volume of the hydride gradually decreases. In other words, when the hydride grows, the ratio R/t, t increases and the oxide can no longer constrain the hydride. Moreover, when the uniform 2D tensile stresses in the oxide disk increase, the elastic strain energy density in the oxide disk increases. One may assume that at some critical size of the hydride the elastic energy will exceed the toughness of the oxide layer and it will break. It is easy to show that the elastic strain energy density in the 2D hydrostatic field is:

$$\frac{E}{V} = \sum_{ij} \frac{\sigma_{ij}\varepsilon_{ij}}{2} = \frac{\sigma_{rr}^2(1-\nu)}{E}.$$

The increase of the stress and the energy with increasing the ratio R/t are described in Fig. 10d.

4. Discussion

We first summarize the experimental evidence and the main results of the theoretical calculations of the elastic fields and energies. Then we shall try to correlate the experimental and the theoretical findings.

4.1. Experimental observations

A few publications [15,22,23] described three stages along the microstructural evolution on the surface of some hydride forming metals exposed to hydrogen at constant pressure. On gadolinium and uranium, many small hydride precipitates ("spots") are nucleated but their growth rate decays and ceases when their diameter reaches less than about 1 μm. Many of the initial hydride precipitates were found to be typical clusters of small precipitates [15]. Sometime after the growth ceases, a few hydrides are observed to grow very rapidly (referred to as "growth centers" [15,22,23]), until they overlap and cover the whole surface.

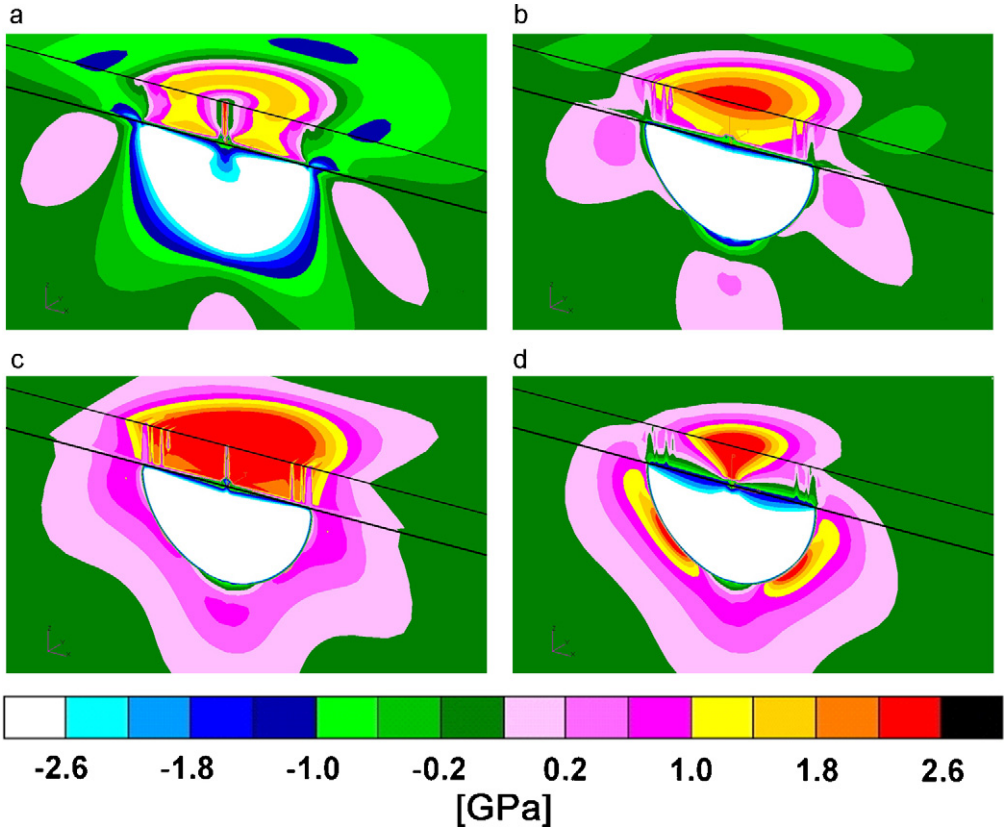

Fig. 9. Stress maps generated by semi-spherical hydride at the proximity of a free surface coated with oxidized film ($R/t = 2.5$). *Anisotropic* material behavior. (a) σ_{rr}, (b) P, (c) $\sigma_{\phi\phi}$ and (d) $\sigma_{\theta\theta}$.

4.2. Mechanical aspects

4.2.1. Stress fields

The stress fields that are generated by a small hydride precipitate that grows below an oxide layer contain in addition to the expected compression regions also regions of *tensile* hydrostatic pressure. These tensile regions are located beneath the hydride particle, penetrating into the metal matrix along the z axis and in side lobes around the hydride. The location and shape of these regions depend on the symmetry of the metal matrix and on the thickness of the oxide layer. They also contain a ring shaped region of compressive hydrostatic stress in the oxide layer. When the hydride grows and the oxide layer thickness becomes negligible, the tensile side lobes expand toward the inner metal space (in the z direction, Fig. 3b) and the slight compressive ring penetrates the matrix around the hydride at the surface region (compare Fig. 7a and b to Fig. 9a and b).

The state of stress in the oxide is a 2D hydrostatic tension. The magnitude of the stress set up in the oxide is smaller, the smaller is the hydride size relative to the oxide thickness (Fig. 10d). The stresses in the oxide are concentrated around the center of the hydride and decay quickly before the hydride–matrix interface is reached (Fig. 9). If two hydrides are growing close to each other, the overlap of the stresses in the oxide due to the two hydrides is small (Fig. 11) thus only if a single hydride particle grows large enough – it may break the oxide.

4.2.2. Energy

When the hydride precipitate is small relative to the oxide thickness (R/t small) it is constrained by the matrix and the relatively rigid oxide and its energy per unit volume is large. As it grows the energy per unit volume of the hydride decreases up to a factor of 2 (Fig. 10c, Section 3.3.2). This property should *enhance the growth rate* with increasing size of the hydride – but this is contrary to the experimental observations that most of the very initial hydride "spots" cease to grow [15,21]!

4.3. Microstructural implications

4.3.1. Initial growth stage-clustering

Unlike the intuitive view, a semispherical dilating hydride particle near a free surface generates lobes of tensile stresses around itself (as explained in Section 3.1.1). The tensile stresses should enhance incoming diffusion of hydrogen toward the hydride and thus enhance its growth rate [25]. The tensile hydrostatic stresses may also serve as traps for hydrogen and favor nucleation of new hydrides at the vicinity of the growing one. Indeed, it has been found that hydrides favorably grow in clusters (Fig. 12).

4.3.2. Cease of growth stage

Cluster formation may, in conditions of limited supply of hydrogen, slow down the growth of the individual hydride precipitates in the colony due to competition on hydrogen. This is probably the case when an oxide layer hinders the incoming diffusion. Another contribution to the slow down of growth is that for a small initial hydride particle, nucleated below a relatively thick oxide layer, a dilative field exists near the topmost metal surface and enhances incoming hydrogen diffusion from the free surface (Section 3.3.1). As the particle grows, the tensile regions move toward the interior and a compressive radial and hydrostatic stresses prevails near the surface that retards further diffusion from the surface (Figs. 7a,b and 9a,b). The deceleration of the growth rate of the initial hydride "spots" may also be due to chemical changes induced by the H_2 gas on the surface of the oxidation overlayer (e.g., formation

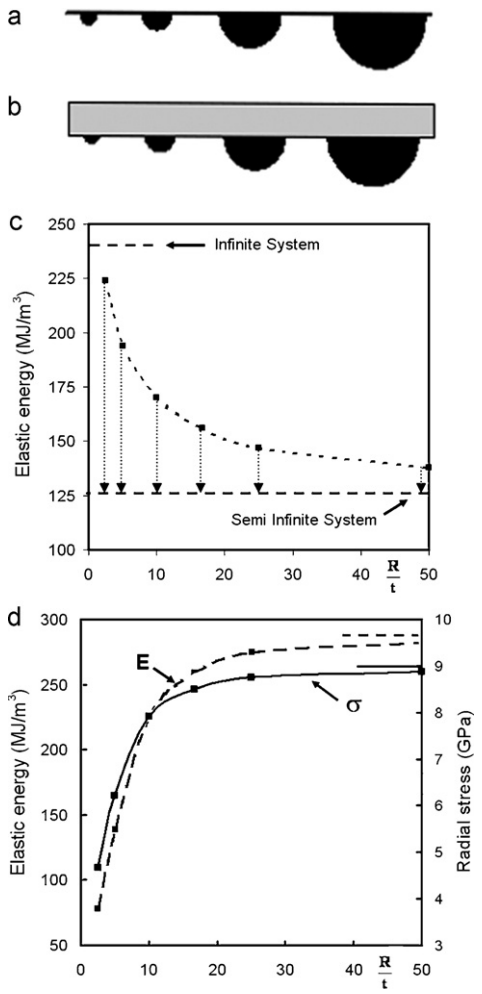

Fig. 10. Evolution of a hydride growing on a free surface, below an oxide layer. (a) A semispherical hydride growing on a free surface. (b) A similar particle growing below an oxide layer. (c) Variation of the total elastic energy of the system, between the limits of the energy of a system without oxide and an infinite matrix. (d) The radial stress and elastic energy density in the disk-shaped *oxide* above the hydride. *R* is the growing hydride radius, *t* is the thickness of the oxide layer. Horizontal lines indicate the stress and energy density when the hydride is infinitely large relative to the oxide film.

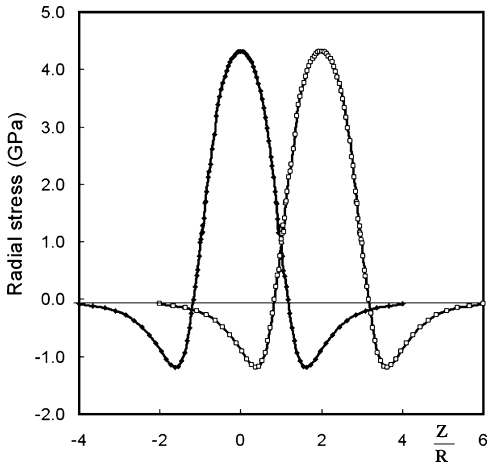

Fig. 11. The profiles of the radial stress generated by two tangent hydride particles in the oxide layer. The overlap of the stresses does not increase the stress beyond the stress at the center above each particle.

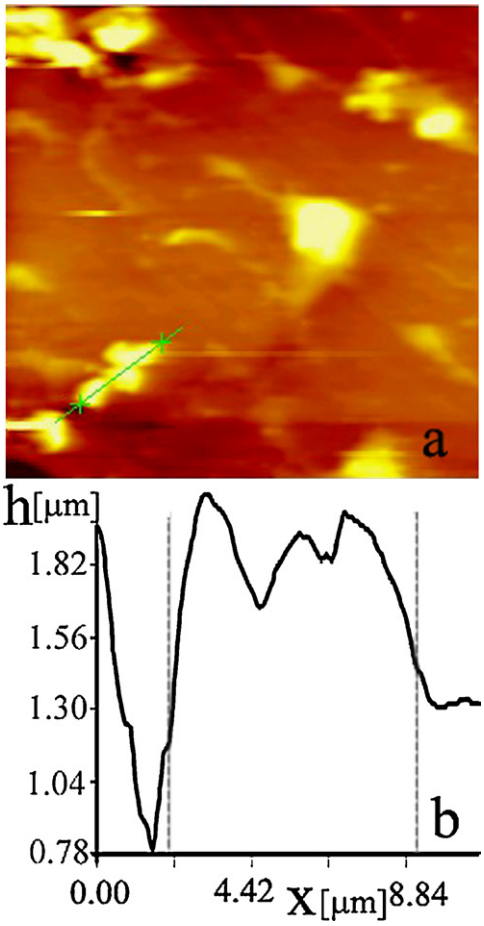

Fig. 12. AFM image of hydride formation on free surface of gadulinium following exposure to 6 mbar H_2 at 250 °C for 8 min. Two clusters are observed in (a), (b) is a line profile of the height across the cluster at the bottom of (a).

of some functional groups such as hydroxyls that impede the dissociative chemisorptions of H_2 [15]). Such changes have not been studied so far, but their occurrence should be considered. Hence the present mechanical analysis just provides one possible mechanism for the slowing down of the growth.

4.3.3. Accelerated growth stage: formation of "growth centers"

As the initial hydrides tend to grow in clusters, no one precipitate grows large enough to break the oxide layer alone and the stress overlap between near hydrides cannot enhance the stress (Fig. 11). Thus which hydride particles continue to grow into a "growth center"? It is observed that hydride particles that grow below incidental defects in the oxide happen to break the oxide and continue to grow [15,22,23]. We suggest that additionally, in most cases only the few hydrides that happen *not to grow in a cluster* – can grow to a size that is large enough to generate the critical stresses in the oxide necessary to break it. Breakage of the oxide gives rise to an abrupt relaxation of the stresses and may restart the growth of a "growth center".

5. Summary

We have calculated and analyzed the elastic fields generated by a hydride particle developing at the near surface region of a metal. Three situations were compared: a spherical hydrides in infinite matrix, a semi spherical hydride on a free surface and the same hydride under an oxide layer. On metal surfaces coated with oxide films, the elastic energy per unit volume of the hydride is maximal

when the hydride is small. The elastic energy per unit volume gradually decreases when the hydride grows relative to the oxide layer thickness, this should in principle, enhance the growth rate of the hydride. Contrary to that, it is observed experimentally that small hydride precipitates nucleate and initially grow rapidly and then cease to grow at some stage. After a while, some of the precipitates start to grow fast in an irregular manner. For these three stages, correlations with the elastic fields are suggested: (a) a hydride particle at a free surface sets up a combination of tensile and compressive hydrostatic stress in the surrounding matrix. This may induce preferred nucleation of new hydrides in the regions of tensile stress and the formation of clusters of hydrides precipitates that is indeed observed experimentally. (b) Clustering, on the other hand, may contribute to the cease of growth due to competition on hydrogen. In addition, as the particle grows, the tensile regions move toward the interior and compressive stresses are set near the surface. This may retard further diffusion from the surface and be another contribution to the cease of growth. (c) A growing hydride increases the stresses in the oxide layer and may finely break it. Then the elastic energy per unit volume of hydrides drops to its minimum value and the growth may accelerate. This formation of a "growth center" is favored when a hydride precipitate grows alone, not in a cluster.

The present work is relating the kinetic and morphological characteristics of the initial hydrides development to the associated mechanical effects. The elastic energy of hydrides and the hydrostatic stress distribution around the hydride may provide the required data for quantitative kinetic analysis (e.g., development of 3D diffusion models). Such analysis is, however, beyond the scope of the present work.

Acknowledgments

The authors acknowledge support by the Germany-Israel Foundation for scientific research. Also partial support has been provided by a grant from the Israel Council for higher education and the Israel Atomic Energy Commission.

References

[1] R. Delmelle, G. Bamba, J. Proost, Int. J. Hydrogen Energy 35 (2010) 9888–9892.
[2] Y. Mishin, W.J. Boettinger, Acta Mater. 58 (2010) 4968–4977.
[3] R. Gremaud, M. Gonzalez-Silveira, Y. Pivak, S. de Man, M. Slaman, H. Schreuders, B. Dam, R. Griessen, Acta Mater. 57 (2009) 1209–1219.
[4] M.X. Gao, S.C. Zhang, H. Miao, Y.F. Liu, H.G. Pan, J. Alloys Compd. 489 (2010) 552–557.
[5] S.L. Li, P. Wang, W. Chen, G. Luo, D.M. Chen, K. Yang, J. Alloys Compd. 485 (2009) 867–871.
[6] R. Balasubramaniam, Acta Metall. 12 (1993) 3341–3349.
[7] B.J. Makenas, H.K. Birnbaum, Acta Metall. 28 (1980) 979–988.
[8] M.P. Puls, Acta Metall. 32 (1984) 1259–1269.
[9] E. Rabkin, V.M. Skripnyuk, Scripta Mater. 49 (2003) 477–483.
[10] A. Pundt, R. Kirchheim, Annu. Rev. Mater. Res. 36 (2006) 555–608.
[11] R.B. Schwarz, A.G. Khachaturyan, Acta Mater. 54 (2006) 313–323.
[12] F.C. Larche, in: J.D. Embury, G.R. Purdy (Eds.), Advances in Phase Transitions, Pergamon, Oxford, 1988, pp. 193–203.
[13] V.P. Zhdanov, Chem. Phys. Lett. 492 (2010) 77–81.
[14] Y. Greenbaum, D. Barlam, M.H. Mintz, R.Z. Shneck, J. Alloys Compd. 452 (2008) 325–335.
[15] G. Benamar, D. Schweke, J. Bloch, T.M. Livneh, H. Mintz, J. Alloys Compd. 477 (2009) 188–192.
[16] N.A.P. Kiran Kumar, J.A. Szpunar, Z. He, J. Nucl. Mater. 403 (2010) 101–107.
[17] M. Martin, C. Gommel, C. Borkhart, E. Fromm, J. Alloys Compd. 238 (1996) 193.
[18] A. Inomata, H. Aoki, T. Miura, J. Alloys Compd. 278 (1998) 103.
[19] G. Liang, J. Huot, S. Boily, R. Schulz, J. Alloys Compd. 305 (2000) 239.
[20] X.H. Guo, S.Q. Shi, Q.M. Zhang, X.Q. Ma, J. Nucl. Mater. 378 (2008) 110–119.
[21] H. Realpe, N. Shamir, Y. Manassen, M.H. Mintz, J. Alloys Compd. 473 (2009) 521–529.
[22] M. Brill, J. Bloch, M.H. Mintz, J. Alloys Compd. 266 (1998) 180–185.
[23] M.H. Mintz, in: K.H.J. Buschow, R.W. Cahn, M.C. Flemings, B. Ilschner, E.J. Kramer, S. Mahajan (Eds.), Encyclopedia of Materials: Science and Technology, Elsevier Science, 2002, pp. 1–9.
[24] J.D. Eshelby, in: Sneddon, Hill (Eds.), Progress in Solid Mechanics, vol. 2, 1961, pp. 89–140 (Eq. (2.43)).
[25] E.C. Aifantis, Acta Mech. 37 (1980) 265–296.
[26] MSC.MARC, The MacNeal-Schwendler Corporation, LA.
[27] D.K. Hsu, R.G. Leisure, Phys. Rev. B 20 (1979) 1339–1344.
[28] N. Xiaoguang, Y.E. Hengqiang, Chin. Phys. Lett. 7 (4) (1990) 188–191.
[29] R. Nunes, et al., ASM handbook, in: Properties and Selection: Nonferrous Alloys and Special-Purpose Materials, vol. 2, ASM International, 1990, p. 715.
[30] R.Z. Shneck, Phil. Mag. A 81 (2001) 383–398.